

Impact of Single Rotations and Entanglement Topologies in Quantum Neural Networks

Marco Mordacci and Michele Amoretti

Quantum Software Laboratory, Department of Engineering and Architecture, University of
Parma, 43124 Parma, Italy
`marco.mordacci1@unipr.it`

Abstract

In this work, an analysis of the performance of different Variational Quantum Circuits is presented, investigating how it changes with respect to entanglement topology, adopted gates, and Quantum Machine Learning tasks to be performed. The objective of the analysis is to identify the optimal way to construct circuits for Quantum Neural Networks. In the presented experiments, two types of circuits are used: one with alternating layers of rotations and entanglement, and the other, similar to the first one, but with an additional final layer of rotations. As rotation layers, all combinations of one and two rotation sequences are considered. Four different entanglement topologies are compared: linear, circular, pairwise, and full. Different tasks are considered, namely the generation of probability distributions and images, and image classification. Achieved results are correlated with the expressibility and entanglement capability of the different circuits to understand how these features affect performance.

1 Introduction

The ability of a variational quantum circuit (VQC) to explore the Hilbert space is measured through the concept of *expressibility* [1]. Another important metric is the *entanglement capability* [1] of the VQC, which measures the ability of the circuit to generate entangled states among qubits. However, high expressibility and high entanglement can lead to barren plateaus [2, 3].

Research about the effect of entanglement has found relevance in VQC [4]. In [5], the authors found that expressibility has a strong correlation with the results achieved, while entanglement capability shows a weaker correlation. In [6], the entanglement production of VQCs is analyzed, and the correlation between expressibility and entanglement is discussed. In [7], an analysis of entanglement and expressibility of different entanglement topologies was performed. The analysis presented in this work goes beyond the scope of [7], providing a broader investigation of entanglement and expressibility across a large set of circuit architectures.

This paper provides the following new contributions: 1) a detailed analysis on the performance of three different tasks, the generation of probability distributions and images and the classification of images, by varying the gates and the entanglement topologies used; 2) a thorough analysis of the performance achieved with respect to entanglement and expressibility values in order to guide the design of VQCs; 3) the execution of the best-performing circuits on real quantum hardware to assess their performance.

The remainder of the paper is organized as follows. In Section 2, the tested circuits, the different metrics, and tasks are presented. In Section 3, the results obtained in the different tasks and the evaluated metrics are presented and discussed. In Section 4, the performance is assessed on real IBM hardware. Finally, Section 5 concludes the paper with a summary of the main results and a discussion of future work.

2 Preliminaries

Two circuit types are considered to investigate how performance is affected by changes in the entanglement topology, the number of circuit layers, the different gates used, and depending on the task to be performed. The first circuit, named C_1 , consists of alternating layers of rotations and entanglement, while the second circuit, named C_2 , follows the same structure as C_1 but with an additional layer of rotations at the end. Four different entanglement topologies, shown in Fig. 1, are considered: linear, circular, full, and pairwise (CNOT is used as

entanglement generator). The considered circuits use 6 qubits because this number of qubits is used for the different tasks tested.

Three tasks are evaluated: the generation of random probability distributions, the generation of images, and the classification of images. The generative tasks are tested with a Quantum Generative Adversarial Network (QGAN) composed of a quantum generator and a classical discriminator, following the structure proposed in [8] for generation of probability distributions, and [9] for the generation of images. Each circuit is tested with 10 random probability distributions, with performance measured by the Hellinger distance between the original and generated distributions.

Image generation is tested using the MNIST dataset, and evaluated by the Fréchet Inception Distance (FID). Additionally, the MNIST dataset is employed for image classification, considering 2 (classes 0-1), 4 (classes 0-3), and 6-class (classes 0-5) classification tasks. Accuracy is used as the evaluation metric. Optimal performance corresponds to lower FID and Hellinger distance, and higher accuracy.

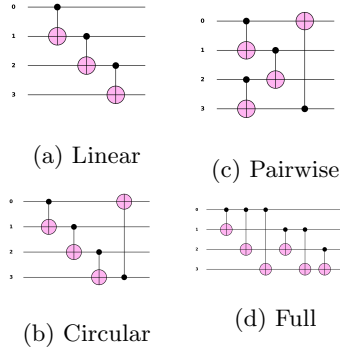


Figure 1: The considered entanglement topologies.

The expressibility, introduced in [1], is calculated as:

$$expr = D_{KL}(P_{VQC}(F; \theta) || P_{Haar}(F)), \quad (1)$$

where D_{KL} is the Kullback-Leibler divergence, F corresponds to the fidelity, P_{VQC} is the estimated probability distribution of fidelities resulting from sampling states from a VQC, and $P_{Haar}(F)$ is the probability density function of fidelities for the ensemble of Haar random states. This measure computes the circuit's ability to generate states that are well representative of the Hilbert space, and it is calculated by comparing the distribution of states obtained from sampling the parameters of a VQC to the uniform distribution, i.e., the ensemble of Haar-random states. A lower expressibility value indicates a higher level of circuit expressiveness.

The entanglement capability [1] is computed as the Meyer-Wallach entanglement measure [10, 11], i.e.,

$$Q(|\psi\rangle) = 2(1 - \frac{1}{n} \sum_{k=0}^{n-1} Tr[\rho_k^2]), \quad (2)$$

where n is the number of qubits. The measure satisfies the following properties: 1) $0 \leq Q(|\psi\rangle) \leq 1$; 2) $Q(|\psi\rangle) = 0$ iff $|\psi\rangle$ is a product state; 3) $Q(|\psi\rangle)$ is invariant under local unitaries.

3 Simulation Results and Analysis of Entanglement and Expressibility

Simulation tests are performed using a Linux machine equipped with an AMD EPYC 7282 CPU and 256 GB RAM.

In all simulations, the combinations of the 3 rotations are not considered since using all of them does not improve the performance. The same results can be produced just by the combination of 2 rotations, as shown in Table 1. This phenomenon likely arises from the fact that the third rotation's effect can be obtained through a combination of the first two rotations.

In [7], the authors take into account only the results of R_x followed by R_y . In this work, all possible combinations of 1 and 2 rotations are considered to understand how the different rotations affect the expressibility and entanglement values.

Circuit	# layer	# rotations	Hellinger	FID	Acc 2C	Acc 4C	Acc 6C
C_1	1	2	0.31	100	99%	61%	41%
		3	0.31	105	99%	61%	41%
	2	2	0.27	45	99%	78%	59%
		3	0.27	45	99%	77%	60%
C_2	1	2	0.24	55	99%	76%	55%
		3	0.25	55	99%	76%	55%
	2	2	0.28	40	99%	84%	68%
		3	0.28	40	99%	85%	70%

Table 1: Comparison between the best performance of the combinations of two and three rotations.

In Figures 2 and 3, the values of the entanglement capability and expressibility are shown. The results illustrate a similar trend for all the combinations of rotations. In particular, the results indicate that the circular topology is the one that produces the highest entanglement, while the full topology generates the lowest entanglement, which seems contradictory since the full topology uses more entangling gates. Moreover, as the number of layers increases, the entanglement capability of the pairwise topology increases until it achieves the highest entanglement, along with the circular configuration. Furthermore, when the number of layers is 1, the linear topology typically exhibits an entanglement value intermediate between the others. However, as the number of layers increases, its value progressively becomes closest to that of the full topology. In any case, with a high number of layers, the entanglement saturates and all topologies converge to similar values. While the circular and pairwise topologies reach an entanglement higher than 0.9 with only 1 or 2 layers (except for R_y), the full and linear need at least 4 layers to generate a similar level of entanglement. Another interesting aspect is that the entanglement values depend not only on the chosen entanglement topology, but also on the individual rotations. R_x rotation generates more entanglement than the R_y . This can be caused by the fact that the R_x rotation depends on the imaginary unit, which adds a phase, while the R_y does not depend on it. The single R_z rotation is ignored since it only adds a phase and does not generate any entanglement.

Regarding expressibility, with C_1 and one layer, when considering each rotational configuration separately, the values are the same for all entanglement topologies. This suggests that expressibility may not depend on the type of entanglement but rather on the rotation used. This is confirmed when the C_2 circuit is considered; indeed, the results for C_2 with 1 layer and C_1 with 2 layers are identical, with one exception: the pairwise topology. The expressibility values of C_2 with x layers are always identical to C_1 with $x+1$ layers. Even though entanglement would constrain the states that the circuit can explore, no distinguishable effect is observed. Moreover, as the number of layers increases, the circular topology exhibits the highest expressibility, followed by the pairwise topology. Nonetheless, when the number of layers increases, the expressibility converges within a range of $10^{-3} \sim 10^{-4}$ and the differences become minimal for all the entanglement topologies; however, the circular and pairwise reach this minimum with 4 layers, while the linear and the full with 6 layers. The single R_z rotation is excluded because, although it provides expressibility similar to that of R_x and R_y , this expressibility is due solely to phase factors and does not lead to good results. The expressibility values, with only one layer of C_1 , are the same for R_x and R_y . However, starting from C_2 and with more layers of C_1 or C_2 , the expressibility values change, and the R_x rotation achieves higher expressibility. This can be due to the phase factor present in R_x and not in R_y .

In Figures 4, 5, 6 and 7, the results achieved by C_1 and C_2 on the various tasks are presented. The binary classification task is omitted, as all configurations have already been shown to easily achieve 99% accuracy (see Table 1). Adam is used (learning rate 0.01, batch size 32, and 5 epochs) to train the network. To encode the images, amplitude embedding is used.

In the context of generation or classification tasks on the MNIST dataset, if a low number of layers is considered, the best entanglement topologies are circular and pairwise, as they achieve the best performance, except for a single layer of C_1 and C_2 where the linear topology achieves comparable results in classification. However, as the number of layers increases, the performance saturates and all topologies perform similarly. This effect is particularly pronounced in the two-rotation combinations.

The generation of probability distributions works slightly better with the linear topology. However, all results are similar from the first layer, except for full topology, which starts to behave similarly from 2 layers for C_1 . All values are approximately 0.35, with only minor variations.

Therefore, when the circuit is simple (a low number of layers) and the task is simple (generation of probability distributions), the linear entanglement performs very well. However, as the task becomes progressively more complex (such as the generation of images) or the circuit becomes more complex (a higher number of layers),

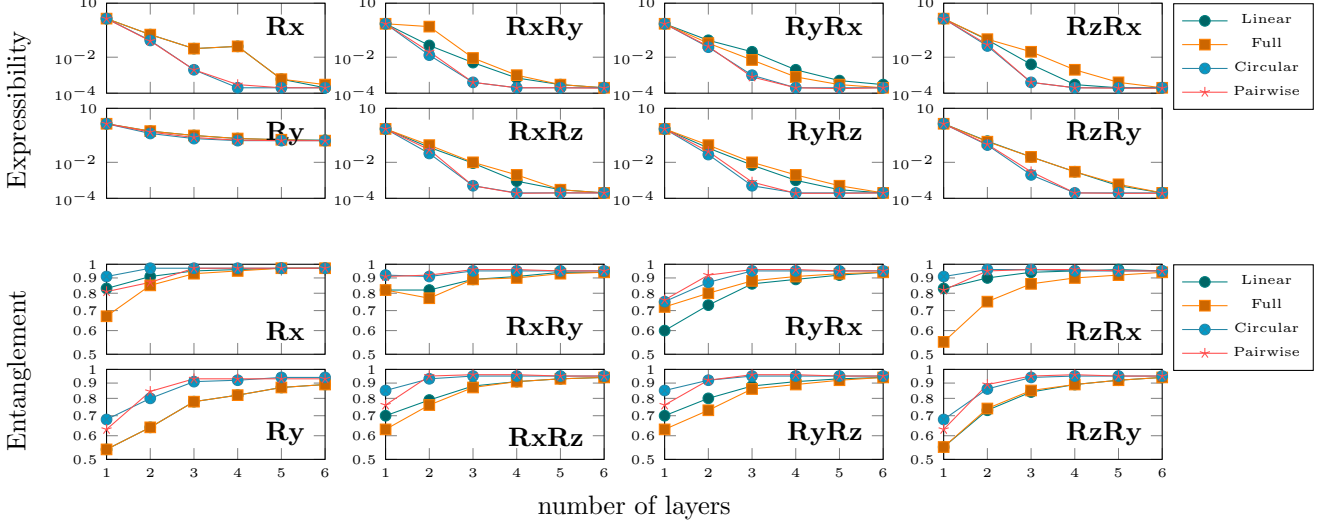


Figure 2: Expressibility and Entanglement of different rotation combinations with circuit C_1 . Expressibility quantified by Kullback-Leibler divergence; lower values mean better expressibility.

the linear topology has deteriorated performance, while the circular and pairwise perform better. Moreover, this is confirmed by the classification task: when using the C_1 circuit with a single layer, the linear topology achieves the best performance along with the circular topology. However, as the number of layers increases, its performance deteriorates.

Therefore, across all tasks, the performance saturates in the same manner as the expressibility and entanglement values. Indeed, starting from 3 layers, the expressibility and entanglement values begin to saturate, and similarly, the performance across the different tasks also saturates. This suggests that, as the number of layers increases, the choice of topology does not affect the performance; therefore, the topology with a lower number of gates should be used. A similar effect seems to occur with the rotations. Starting from 3 layers, the different rotation configurations reach a similar level of expressibility and entanglement and the same happens to the performance. Then, the choice of different rotations seems almost useless.

An additional interesting aspect emerges when the individual rotation configurations are considered with a low number of layers. In both image generation and classification, the single R_y rotation performs better than the R_x rotation, while in the probability distribution task, the R_x rotation achieves better results. Therefore, this may suggest that with image-based tasks, R_y performs better; however, this has to be investigated further, as it could be specific to the MNIST dataset. Furthermore, in image-based tasks, the pairwise topology seems to perform better. This could be due to its ability to connect neighboring qubits and, consequently, neighboring pixels.

Additionally, the combinations of R_x and R_y rotations generally perform better with a lower number of layers. This suggests that adding a phase using the R_z rotation is not particularly useful or at least not as effective as the rotations on the x and y axes. The addition of a R_x or R_y gate always improves the performance, while the R_z gate does not. It is understandable when R_z is applied as the first rotation to the $|0\rangle$ state, as it only adds a phase to $|0\rangle$. However, there are cases where it performed well with image tasks. For instance, in the classification tasks, all combinations of the two rotations, except for the R_xR_z rotational layer, performed similarly, although the R_xR_y and R_yR_x are the most consistent and they are the combinations with the highest and lowest entanglement values, respectively; thus, higher entanglement does not appear to be an issue, even though barren plateaus should be studied [3].

Furthermore, when considering the circuit C_1 with a single rotation configuration and two layers, it leads to better expressibility values compared to the two-rotation configurations with only a single layer, which have the same number of parameters, although both configurations have similar entanglement values. However, this higher expressibility of the two-layer circuits leads to worse performance with respect to the one-layer circuits in all tasks. Therefore, having a high expressibility is ineffective if the circuit does not also enhance its entanglement capability.

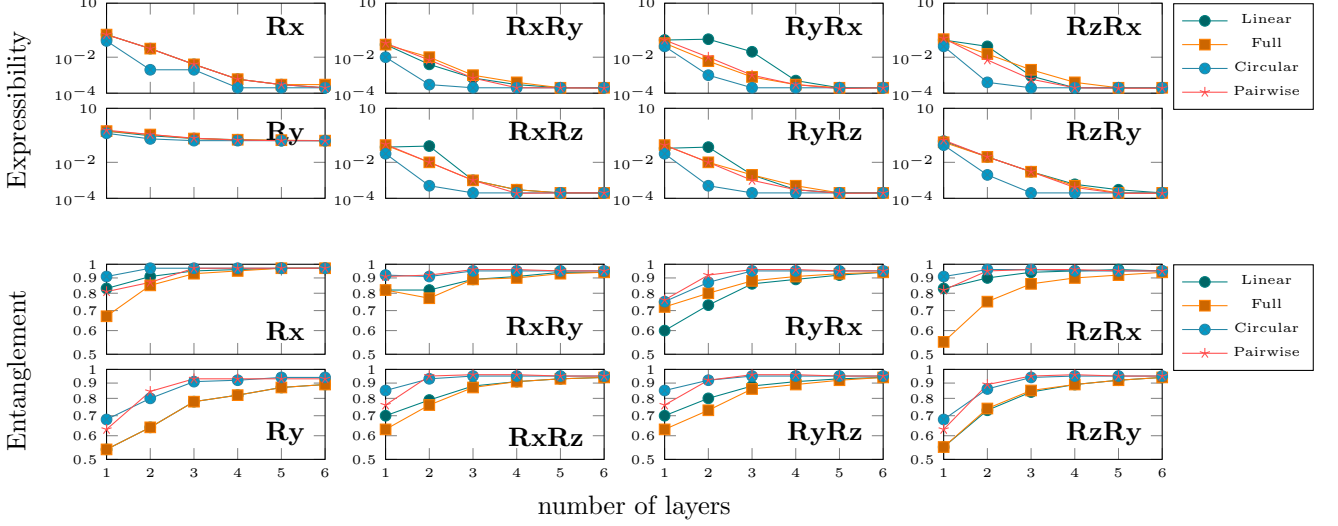


Figure 3: Expressibility and Entanglement of different rotation combinations with circuit C_2 . Expressibility quantified by Kullback-Leibler divergence; lower values mean better expressibility.

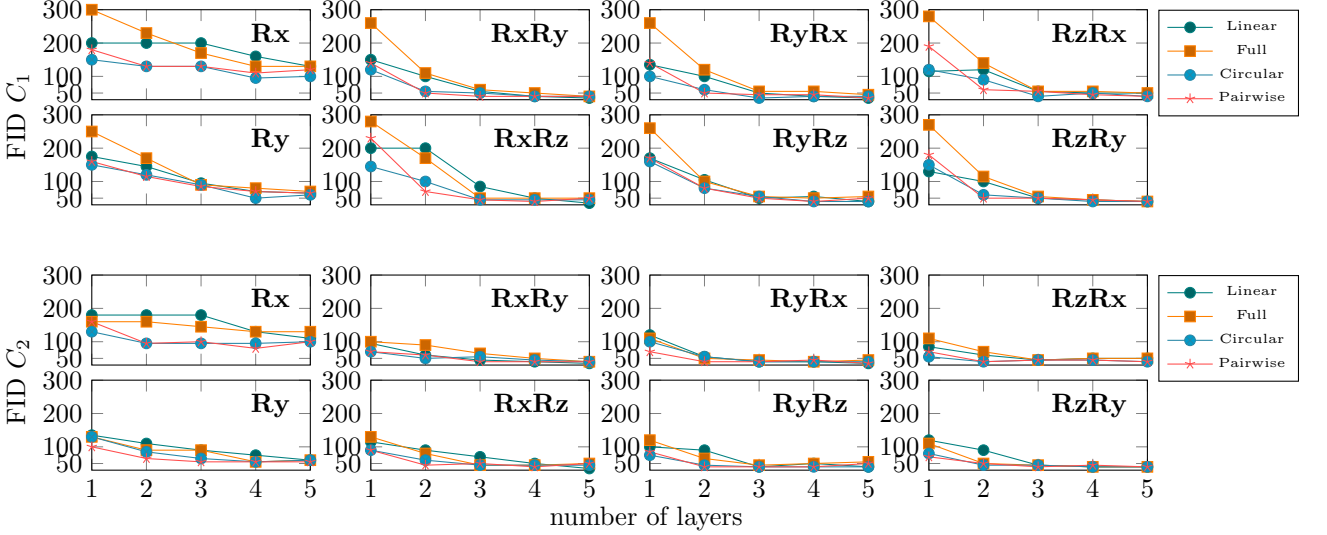


Figure 4: FID results of C_1 and C_2 .

4 Execution on Real Quantum Computers

The best-performing circuits between the execution with a low number of layers for each task are also tested on real IBM hardware to assess their performance. In particular, the generation of probability distributions is tested with R_x rotation and with linear topology with only a single layer of C_1 . The generation of images is tested with $R_x R_y$ combinations, with the circular topology and two layers. The 2/4-class classifications are tested, respectively, with: a single layer of the C_1 circuit with an R_y gate and circular topology, and two layers of the C_1 circuit with $R_x R_y$ gates and circular topology.

Tables 2 and 3 report the QNN results. The tests are performed with 1024 shots. The MNIST testset is used to assess classification performance, while 30 random probability distributions and 100 fake images are used for QGAN tasks. The performance achieved on the real hardware is quite similar to that obtained in simulation, except for the classification task. In particular, the probability distribution task achieves a Hellinger distance of 0.35 (vs. 0.31 in simulation). The generation of images obtains a FID score of 80 (vs. 55). In contrast, classification accuracy drops significantly: 56% (vs. 99%) for two classes, and 40% (vs. 78%) for four. This discrepancy is mainly due to the amplitude encoding used to map images into quantum states. This encoding method significantly increases the depth of the quantum circuit compared to the two generative tasks.

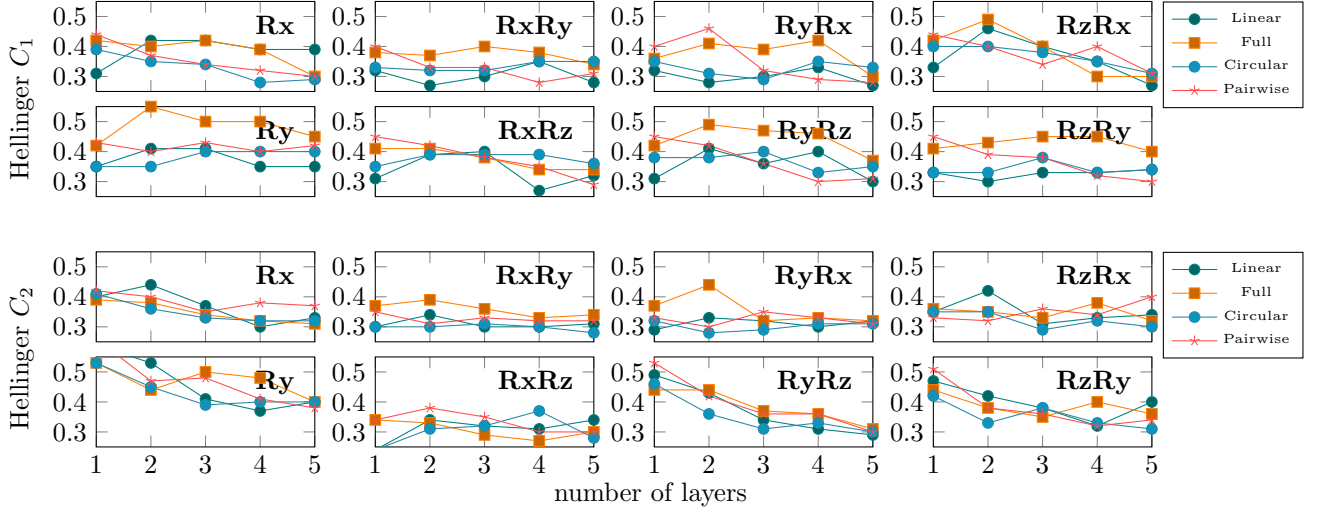


Figure 5: Hellinger distance results of C_1 and C_2 .

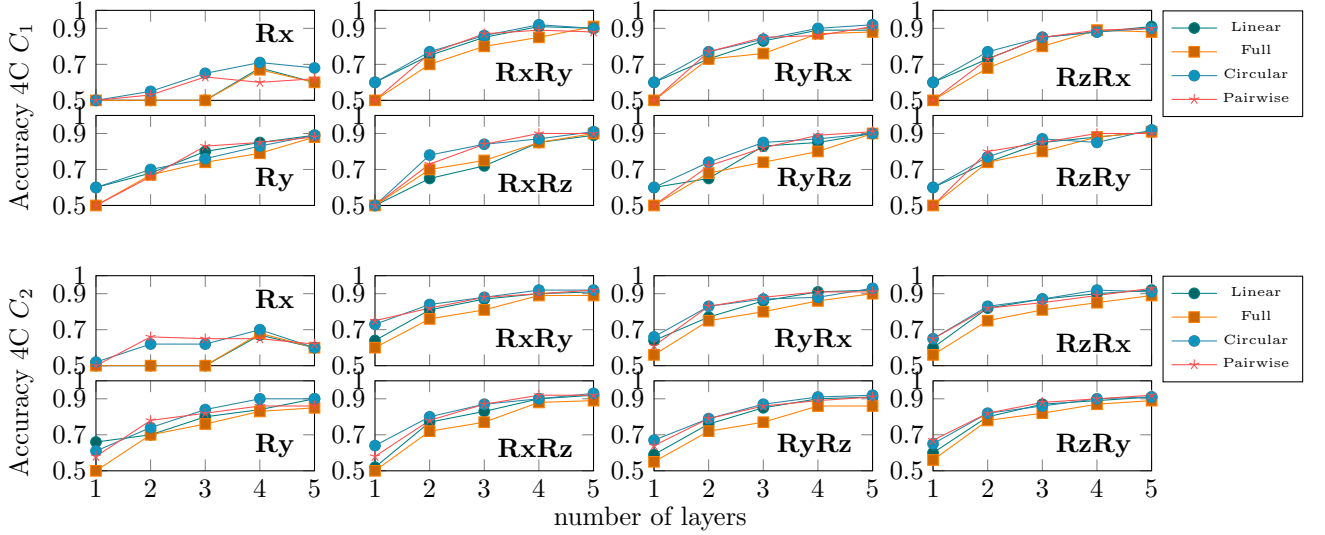


Figure 6: Classification accuracy results of C_1 and C_2 with 4 classes.

5 Conclusion

In this work, an analysis of the performance of various VQCs is performed using two types of circuits: one with alternating rotations and entanglement layers, and another with an additional final rotations layer. The investigation explores different entanglement topologies (linear, circular, pairwise, and full), gate configurations (single and two-rotations), QML tasks (probability distribution generation, image generation, classification), and the number of layers.

The performance achieved in the three tasks is correlated with entanglement and expressibility. With few layers, $R_x R_y$ and $R_y R_x$ configurations consistently perform best, and with circular or pairwise topologies, while the full topology performs worse. Furthermore, when evaluating the circuits as a whole, with a low number of layers, the performance appears to depend more on the entanglement topology. Linear and full topologies exhibit lower entanglement and expressibility values and perform poorly, while circular and pairwise have a slightly higher entanglement and expressibility and achieve better results. However, as the number of layers increases, all topologies achieve comparable expressibility and entanglement, leading to similar performance saturation across all tasks. The same trend is observed with the rotations: as the number of layers increases, the performance of the different two-rotation configurations is similar and saturates, such as expressibility and entanglement. Moreover, when using two-rotation configurations, with a low number of layers, considering the entanglement topologies separately, the best results are obtained with either the highest or lowest entanglement

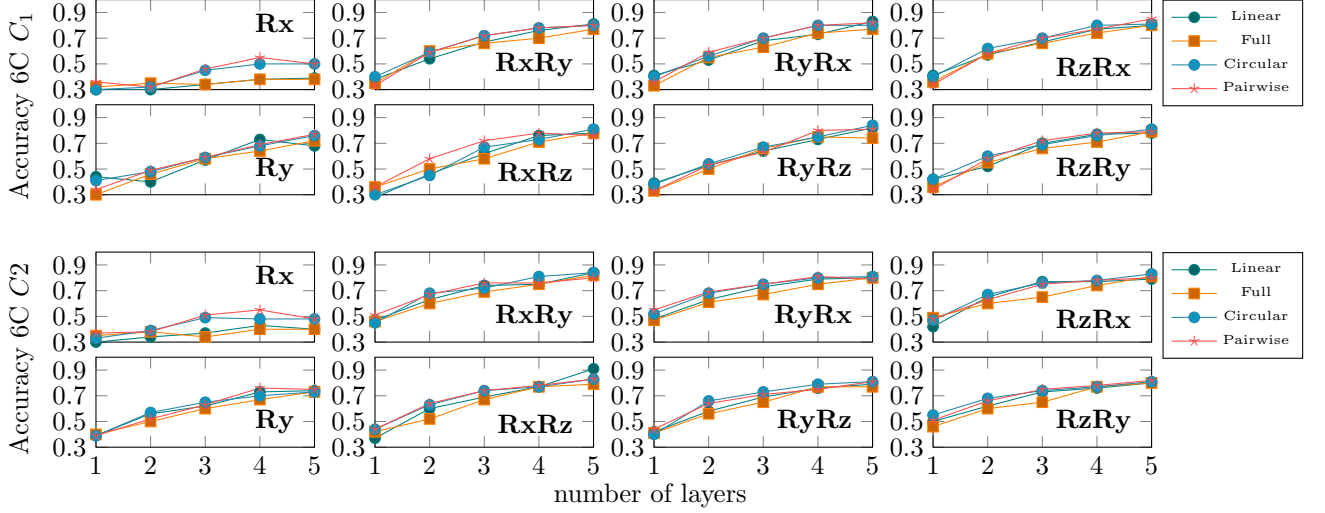


Figure 7: Classification accuracy results of C_1 and C_2 with 6 classes.

Task	Circuit	Rot Gate	# layer	Ent topology	IBM Fez	IBM Mar-rakesh	IBM Kingston
QGAN Probs	C_1	R_x	1	Linear	0.34	0.36	0.35
2 Classes	C_1	R_y	1	Circular	56%	50%	47%

Table 2: Results on real IBM quantum computers. Metrics: Hellinger distance for QGAN and accuracy for classification.

or expressibility. Additionally, each task is tested on real IBM hardware to assess performance.

Future work will validate these findings across diverse tasks and datasets to assess their generalizability. The impact of Barren Plateaus will be considered. Furthermore, evaluating circuits with more qubits will help to verify the consistency of the results. Moreover, exploring mixed-gate layers and different entangling gates may also clarify the dependence of performance on specific gate choices.

Acknowledgment

We acknowledge the financial support from Spoke 10 - ICSC - “National Research Centre in High Performance Computing, Big Data and Quantum Computing”, funded by European Union – NextGenerationEU. This research benefits from the High Performance Computing facility of the University of Parma, Italy (HPC.unipr.it) and also from IBM Quantum Credits awarded to Michele Amoretti - project Crosstalk-aware Quantum Multi-programming.

Task	Circuit	Rot Gate	# layer	Ent topology	IBM Mar-rakesh
QGAN Images	C_1	$R_x R_y$	2	Circular	80
4 Classes	C_1	$R_x R_y$	2	Circular	40%

Table 3: Results on real IBM quantum computer. Metrics: FID for QGAN and accuracy for classification.

References

- [1] Sukin Sim, Peter D Johnson, and Alán Aspuru-Guzik. Expressibility and entangling capability of parameterized quantum circuits for hybrid quantum-classical algorithms. *Advanced Quantum Technologies*, 2(12):1900070, 2019.
- [2] Zoë Holmes, Kunal Sharma, Marco Cerezo, and Patrick J Coles. Connecting ansatz expressibility to gradient magnitudes and barren plateaus. *PRX quantum*, 3(1):010313, 2022.
- [3] Carlos Ortiz Marrero, Mária Kieferová, and Nathan Wiebe. Entanglement-induced barren plateaus. *PRX quantum*, 2(4):040316, 2021.
- [4] Joonho Kim and Yaron Oz. Entanglement diagnostics for efficient vqa optimization. *Journal of Statistical Mechanics: Theory and Experiment*, 2022(7):073101, 2022.
- [5] Thomas Hubregtsen, Josef Pichlmeier, Patrick Stecher, and Koen Bertels. Evaluation of parameterized quantum circuits: on the relation between classification accuracy, expressibility, and entangling capability. *Quantum Machine Intelligence*, 3(1):9, 2021.
- [6] Marco Ballarín, Stefano Mangini, Simone Montangero, Chiara Macchiavello, and Riccardo Mengoni. Entanglement entropy production in quantum neural networks. *Quantum*, 7:1023, 2023.
- [7] Guilherme Ilário Correr, Ivan Medina, Pedro C Azado, Alexandre Drinko, and Diogo O Soares-Pinto. Characterizing randomness in parameterized quantum circuits through expressibility and average entanglement. *Quantum Science and Technology*, 10(1):015008, 2024.
- [8] Christa Zoufal, Aurélien Lucchi, and Stefan Woerner. Quantum generative adversarial networks for learning and loading random distributions. *npj Quantum Information*, 5(1):103, 2019.
- [9] He-Liang Huang, Yuxuan Du, Ming Gong, Youwei Zhao, Yulin Wu, Chaoyue Wang, Shaowei Li, Futian Liang, Jin Lin, Yu Xu, et al. Experimental quantum generative adversarial networks for image generation. *Physical Review Applied*, 16(2):024051, 2021.
- [10] David A Meyer and Nolan R Wallach. Global entanglement in multiparticle systems. *arXiv preprint quant-ph/0108104*, 2001.
- [11] Gavin K Brennen. An observable measure of entanglement for pure states of multi-qubit systems. *arXiv preprint quant-ph/0305094*, 2003.